MOLECULAR AND CELLULAR BIOLOGY, Dec. 2005, p. 11005–11018 Vol. 25, No. 24
0270-7306/05/$08.00+0 doi:10.1128/MCB.25.24.11005–11018.2005

Endosomal Transport of ErbB-2: Mechanism for Nuclear Entry of the Cell Surface Receptor†

Dipak K. Giri,‡ Mohamed Ali-Seyed,‡ Long-Yuan Li,‡ Dung-Fang Lee, Pin Ling, Geoffrey Bartholomeusz, Shao-Chun Wang, and Mien-Chie Hung*

Department of Molecular and Cellular Oncology, University of Texas M. D. Anderson Cancer Center, Houston, Texas 77030

Received 20 April 2005/Returned for modification 3 June 2005/Accepted 21 September 2005

The cell membrane receptor ErbB-2 migrates to the nucleus. However, the mechanism of its nuclear translocation is unclear. Here, we report a novel mechanism of its nuclear localization that involves interaction with the transport receptor importin β1, nuclear pore protein Nup358, and a host of players in endocytic internalization. Knocking down importin β1 using small interfering RNA oligonucleotides or inactivation of small GTPase Ran by RanQ69L, a dominant-negative mutant of Ran, causes a nuclear transport defect of ErbB-2. Mutation of a putative nuclear localization signal in ErbB-2 destroys its interaction with importin β1 and arrests nuclear translocation, while inactivation of nuclear export receptor piles up ErbB-2 within the nucleus. Additionally, blocking of internalization by a dominant-negative mutant of dynamin halts its nuclear localization. Thus, the cell membrane-embedded ErbB-2, through endocytosis using the endocytic vesicle as a vehicle, importin β1 as a driver and Nup358 as a traffic light, migrates from the cell surface to the nucleus. This novel mechanism explains how a receptor tyrosine kinase on the cell surface can be translocated into the nucleus. This pathway may serve as a general mechanism to allow direct communication between cell surface receptors and the nucleus, and our findings thus open a new era in understanding direct trafficking between the cell membrane and nucleus.

Despite a number of recent reports on translocation of receptor tyrosine kinases (RTKs) to the nucleus (reviewed in references 8 and 52), the mechanism of how RTKs travel from the cell surface to the nucleus is still unknown. Transmembrane receptors serve as sensors, recognizing the growth factor in the extracellular environment and conveying the message through the signaling cascade to the nucleus. However, some RTKs, like the epidermal growth factor receptor (EGFR) family members (27, 29, 32, 36, 37, 49, 54), fibroblast growth factor receptor 1 (FGFR1) and FGFR3 and their splice variants (23, 31, 40, 43, 44, 45, 57), insulin receptor (41), and vascular endothelium growth factor receptor Flk1/KDR (13, 21, 34), are known to migrate to the nucleus either intact or as a fragment of proteolytic cleavage, interestingly, with or without the corresponding ligand. These nuclear RTKs have been shown to act as transcription factors (27, 36, 49, 54) for genes like *Cyclin D1* (27), *FGF2* (38), and *COX-2* (49) and modulators for induction of c-jun and cyclin D1 (40). Additionally, nuclear matrix binding of FGFR1 and insulin receptor (41, 45) has been shown to strategically position the receptors for involvement in the regulation of gene expression. More recently, the nuclear EGFR was shown to interact with well-known DNA binding transcriptional factors, such as STAT3 and E2F1, to regulate the expression of inducible nitric oxide synthase and B-Myb (17, 28). Overall, these reports support direct roles for RTKs in the nucleus, which represent a new class of RTK functions. However, the mechanism of their nuclear import is virtually unknown. We report here on a novel transport mechanism leading to nuclear entry of cell membrane ErbB-2.

* Corresponding author. Mailing address: Department of Molecular and Cellular Oncology, University of Texas M. D. Anderson Cancer Center, 1515 Holcombe Boulevard, Box 79, Houston, TX 77030. Phone: (713) 792-3668. Fax: (713) 794-0209. E-mail: mhung@mdanderson.org.

† Supplemental material for this article may be found at http://mcb.asm.org/.

‡ These authors contributed equally.

MATERIALS AND METHODS

Cell culture and antibodies. All cell lines were maintained in Dulbecco modified Eagle medium–F-12 with 10% fetal bovine serum. The antibodies used in this study were as follows: anti-ErbB-2 (Oncogene); anti-dynamin 2, anti-EPS15, mouse immunoglobulin G1 (IgG1), mouse IgG2a, anticlathrin, and anti-poly(ADP-ribose) polymerase (anti-PARP; BD Biosciences); antiadaptin (Affinity Bioreagents); anti-importin β1 and anticalreticulin (Santa Cruz Biotechnology); anti-EEA1 and antiphosphotyrosine (Upstate Biotechnology Inc.); anti-α-tubulin and anti-Flag (Sigma); anti-green fluorescent protein (anti-GFP; NeoMarkers); and anti-histone H3 (Cell Signaling). All the secondary antibodies were obtained from Vector Laboratories and Jackson ImmunoResearch.

Cellular fractionation. Cellular fractionation was performed as described previously (16, 27). Briefly, cells were washed twice with phosphate-buffered saline (PBS) and resuspended in buffer A (50 mM NaCl, 10 mM HEPES, pH 8.0, 500 mM sucrose, 1 mM EDTA, 0.2% Triton X-100, 0.5 mM 2-mercaptoethanol, 1 mM NaF, 1 mM Na_3VO_4, 1 mM phenylmethylsulfonyl fluoride [PMSF], and 2 μg/ml aprotinin) for 15 min on ice. Cells were homogenized with 20 strokes using a Dounce homogenizer. An aliquot of cells was checked for cell lysis under the microscope by addition of trypan blue to confirm that >98% of cells were lysed. After brief centrifugation, the supernatant was collected as a cytoplasmic fraction and the pelleted nuclei were further washed three times with isotonic sucrose buffer (250 mM sucrose, 6 mM $MgCl_2$, 10 mM Tris-HCl, pH 7.4) containing 0.5% nonionic detergent Triton X-100 to dissolve any cytoplasmic membrane contaminants. The purity of the nuclei was evaluated under the microscope by staining the nuclei with 1% methylene blue; the nuclei were clean, with no membrane sticking to the outside of the nucleus (16). To extract nuclear proteins, the isolated nuclei were resuspended in buffer C (350 mM NaCl, 10 mM HEPES, pH 8.0, 25% glycerol, 0.1 mM EDTA, 0.5 mM 2-mercaptoethanol, 1 mM PMSF, and 2 μg/ml aprotinin) with gentle rocking for 30 min at 4°C. After centrifugation, the supernatant was collected as a nuclear fraction. The fractionation efficiency was also analyzed using antibodies against α-tubulin, histone H3, or PARP.

Transfection, immunoprecipitation, and immunoblotting. Cells were transfected using the liposome delivery system. Briefly, cells were grown on petri dishes or slides overnight and incubated with plasmid/liposome complex in the serum-free medium for 5 to 6 h followed by replacement of serum-containing

medium and incubation at 37°C for 16 to 24 h. In some cases cells were transfected using electroporation (Amaxa Biosystems). For small interfering RNA (siRNA) transfection, siRNA oligonucleotides targeting importin β1 and nonspecific siRNA oligonucleotides were purchased from Dharmacon. The siRNA oligonucleotides were transfected into MCF-7/HER18 cells using liposome according to the standard protocol as provided by Dharmacon. Seventy-two hours after transfection, cells were harvested and analyzed by Western blotting.

For coimmunoprecipitation experiments, cellular extracts were lysed in lysis buffer (150 mM NaCl, 1 mM EDTA, 20 mM Tris, pH 7.5, 0.5% NP-40, 1 mM NaF, 1 mM Na_3VO_4, 1 mM PMSF, and 2 μg/ml aprotinin) and incubated with primary antibodies at 4°C followed by incubation with protein G-Sepharose or protein A-Sepharose (Roche). The immunocomplexes were washed three times with lysis buffer. For single immunoprecipitation, the bound proteins were eluted by boiling the samples in sodium dodecyl sulfate (SDS) sample buffer containing 2-mercaptoethanol. For sequential double immunoprecipitation, the bound proteins were eluted from the Sepharose beads by being boiled for 3 min in 25 μl of SDS lysis buffer (20 mM Tris, pH 7.5, 50 mM NaCl, 1% SDS, and 1 mM dithiothreitol) (24). Samples were cooled down, and the supernatant was diluted with 225 μl of lysis buffer containing appropriate antibodies and incubated overnight at 4°C. The immunocomplexes were then precipitated with protein A-Sepharose, washed with lysis buffer, and resuspended in SDS sample buffer. The eluted proteins were boiled for 5 min and subjected to SDS-polyacrylamide gel electrophoresis.

Plasmids and luciferase reporter assay. For constructing ErbB-2hGFP, a PCR fragment of the C-terminal end of ErbB-2 was generated using the pcDNA3-ErbB-2 as template. The 5′ primer, 5′-CCGGGAAAACCGCGGACGCCTGGG CTCCCAGGACCTGCTGAACTGGTG-3′, was designed to extend from bp 2604 to 2652. The 3′ primer, 5′-GCGAGTCTCGAGCACTGGCACGTCCAG-3′, was designed to delete the stop codon of ErbB-2. This 1,383-bp ErbB-2 product missing the stop codon was used to replace the corresponding sequence within the wild-type (WT) ErbB-2 cDNA sequence. For the expression of ErbB-2hGFP-tagged fusions, the HindIII/XhoI ErbB-2 fragment from pcDNA3-ErbB-2 was cloned into the corresponding sites in the phrGFP-C mammalian expression vector (Stratagene). The mutant ErbB-2ΔNLS was generated by deleting the putative nuclear localization signal (NLS) sequence (amino acids [aa] 676-KRRQQKIRKYTMRR-689), which resulted in the sequence of KLM at the deletion junction. N-terminal (aa 1 to 675) and C-terminal (aa 690 to 1234) portions of ErbB-2 were PCR amplified using a high-fidelity PCR kit (Roche) and two sets of primers, 5′-ATCGCTAGCATGGAGCTGGCGGCCTTG-3′ with 5′-ATCAAGCTTGATGAGGATCCCAAAGAC-3′ and 5′-ATCAAGCTT ATGCTGCTGCAGGAAACGGAG-3′ with 5′-ATCACCGGTAACACTGGC ACGTCCAGACC-3′, respectively. The amplified N-terminal portion that contains NheI (5′ end) and HindIII (3′ end) and the C-terminal portion that contains HindIII (5′ end) and AgeI (3′ end) were digested and sequentially cloned into the pEGFP-N1 vector (BD Biosciences). DNA fragments encoding the Flag-tagged WT Ran or RanQ69L mutant were amplified by PCR using pQE-Ran and pQE-RanQ69L (35) as templates, respectively, and cloned into the pcDNA3 vector. The pQE-Ran and pQE-RanQ69L plasmids were a generous gift from Karsten Weis. GFP-tagged dynamin 2 (6), dominant-negative mutant K44A (7), and GFP-tagged EPS15 (3) were kindly provided by Mark A. McNiven and Alexandre Benmerah. The nucleotide sequences of all constructs were confirmed by direct DNA sequencing.

For luciferase reporter assays, the GFP-tagged WT or ΔNLS ErbB-2 mutant or vector control was cotransfected with the Elk1 fusion transactivator plasmid (pFA2-Elk1; Stratagene) and luciferase reporter plasmid pFR-Luc (Stratagene), respectively. As a transfection efficiency control, the *Renilla* luciferase reporter plasmid pRL-TK (Promega) was also cotransfected into cells. Twenty-four hours after transfection, the cells were treated with or without tyrosine kinase inhibitor AG825 (80 μM) for 6 h. Luciferase assays were carried out using the Dual-Luciferase assay kit (Promega) as specified by the manufacturer. The luciferase activity induced by the vector alone without AG825 treatment was set as 100%, and the relative luciferase activities were presented as the mean with standard deviation of three independent experiments performed in triplicate.

Immunofluorescence. Cultured cells were fixed with 4% paraformaldehyde for 15 min, permeabilized on ice with 0.1% Tween 20 for 5 min, and then immunostained using primary antibodies for 1 h at 37°C. After three washes with PBS, the fluorescein isothiocyanate-conjugated secondary antibody was then applied for 45 min at room temperature. The nucleus was stained with DAPI (4′,6′-diamidino-2-phenylindole; fluorescence) or TOPRO 3 (confocal) before mounting. The fluorescence images were captured with a Zeiss AxioPlan2 fluorescence microscope equipped with a digital camera. A Zeiss CLM510 laser microscope performed the confocal analysis.

Transmission electron microscopy. The cells were scraped, washed with filtered PBS, syringed to get single-cell suspensions, spun down, and fixed in 0.4% glutaraldehyde in 0.1 M phosphate buffer (pH 7.4) for 1 h at room temperature. After being washed three times with PBS, cells were treated with 2% osmium tetroxide in PBS, dehydrated in an ascending series of ethanol, and sequentially infiltrated with araldite-ethanol (1:1) for 2 h, araldite-ethanol (4:1) overnight, araldite for 45 min at 45°C, araldite for 45 min at 55°C, and finally araldite to a depth of 1.5 to 2 mm before polymerization at 60°C for 24 h. Ultrathin sections of cells were prepared using an ultramicrotome (Reichert E), mounted on the copper grids, and treated with sodium metaperiodate for 30 min followed by 5% normal goat serum treatment for 30 min, followed by presaturation with either mouse or rabbit IgG (rIgG) before being treated with specific primary antibodies. Sections were then incubated for 45 min with gold particles labeled with goat anti-mouse or anti-rabbit secondary antibody (Amersham Biosciences). Sections were washed and stained with uranyl acetate for 2 min and Reynolds' lead citrate for 1 min before examination on a JEOL 1200EX microscope.

RESULTS

Importin β1 is required for ErbB-2 nuclear translocation. The nuclear import mechanism depends on interactions between the transport receptors importins or karyopherins, nuclear pore proteins and their targeting sequences, and the NLS carried by the cargoes (reviewed in reference 51). Since nuclear transport of cargoes depends on association with transport receptors of the importin β family (reviewed in reference 46), we explore the possibility of ErbB-2 being associated with importin β1. Cytoplasmic extracts from different breast cancer cell lines were immunoprecipitated using an anti-ErbB-2 antibody followed by Western blot analysis using anti-importin β1 antibody. Interaction between ErbB-2 and importin β1 was detected in the cytoplasmic extracts of ErbB-2-overexpressing MDA-MB-453 and MCF-7/HER18 cells (4, 49) but not those of MCF-7 cells, which express basal levels of ErbB-2 (Fig. 1A, upper panel). The same results were observed by a reciprocal immunoprecipitation and Western blot analysis (IP-WB) using anti-importin β1 and anti-ErbB-2 antibody, respectively (Fig. 1A, lower panel). Also, the importin β1–ErbB-2 interaction occurred in the nucleus as revealed by IP-WB using nuclear lysates from these cell lines (Fig. 1B). Thus, as with other proteins that enter the nucleus via interaction with importin β1, the interactions between importin β1 and ErbB-2 can be detected in both the cytoplasm and the nucleus (reviewed in references 15, 30, and 33). These biochemical results are consistent with the immunofluorescence studies, in which colocalization of ErbB-2 and importin β1 was detected in the cytoplasm and nucleus by confocal microscopy (Fig. 1C, insets 1 and 2). The potential interference from endoplasmic reticulum contamination was ruled out by staining the cells for the endoplasmic reticulum marker calreticulin (data not shown). Ultrastructural studies using electron microscopy further confirmed the ErbB-2 and importin β1 association in cellular compartments including the cytoplasm and the nucleus. The gold particles labeling ErbB-2 (15 nm) and importin β1 (5 nm) were detectable when the specific primary antibodies against ErbB-2 and importin β1 were treated (Fig. 1D). Without treatment of specific primary antibodies, gold particles were not detected even in the presence of gold particle-labeled secondary antibodies (data not shown), indicating the specificity of the detected gold particles. Thus, the interaction between ErbB-2 and importin β1 can be detected in both the cytoplasm and the nucleus by three different methods, suggesting the possibility that importin β1 may be involved in ErbB-2 nuclear

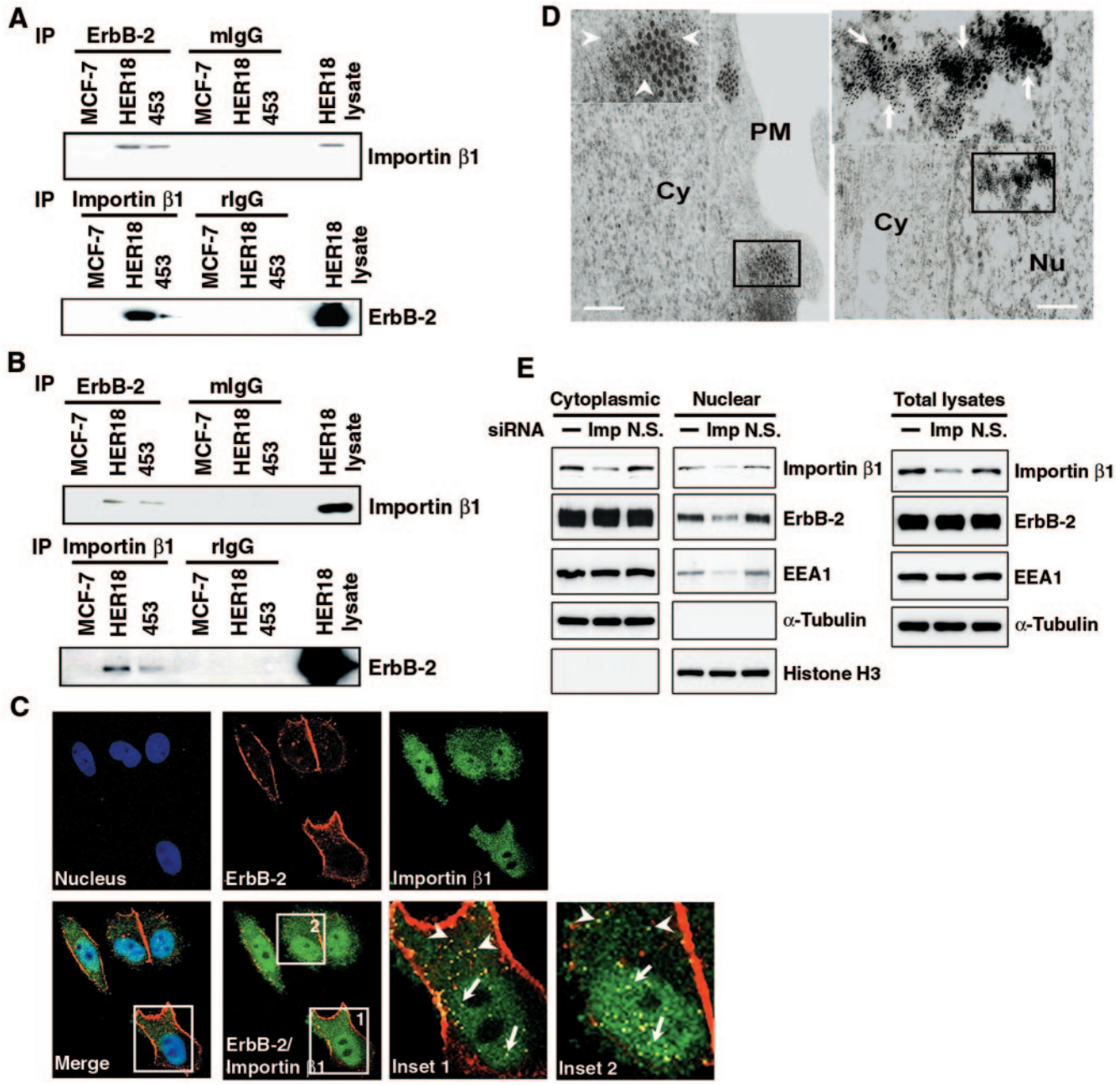

FIG. 1. ErbB-2 interacts with importin β1. (A) Lysates of the cytoplasmic fraction from MCF-7, MCF-7/HER18, and MDA-MB-453 cells were immunoprecipitated (IP) with antibodies against ErbB-2, importin β1, control mouse IgG (mIgG), and rIgG. The presence of importin β1 and ErbB-2 in the immunocomplexes was examined by immunoblotting analysis. Total cell lysate from the MCF-7/HER18 cells was used as the positive control. (B) Nuclear lysates from the same cell lines were tested for the association between ErbB-2 and importin β1 as described for panel A. Total cell lysate from the MCF-7/HER18 cells was used as the positive control. (C) ErbB-2 and importin β1 colocalized in the cytoplasm (insets 1 and 2, arrowheads) and the nucleus (insets 1 and 2, arrows) of MCF-7/HER18 cells as shown by immunofluorescence staining using a mouse monoclonal anti-ErbB-2 antibody directed against the extracellular domain of ErbB-2 and a rabbit polyclonal anti-importin β1 antibody. The images were then analyzed by confocal microscopy. The boxed areas are shown in detail in insets 1 and 2. (D) Immunogold staining of ultrathin sections for ErbB-2 and importin β1 demonstrated their association in the cytoplasm (left, inset, arrowheads) and nucleus (right, inset, arrows) of MCF-7/HER18 cells. The large and small gold particles labeled ErbB-2 (15 nm) and importin β1 (5 nm), respectively. Bar = 200 nm. Cy, cytoplasm; Nu, nucleus; PM, plasma membrane. (E) MCF-7/HER18 cells were transfected with importin β1 siRNA (Imp), nonspecific siRNA control (N.S.), or buffer only (−). Proteins from the cytoplasmic, nuclear, and total cell lysates were then analyzed by Western blotting with antibodies as indicated.

transport. To address this issue, we asked whether importin β1 may be required for ErbB-2 nuclear import. We used the siRNA approach to specifically knock down importin β1 expression in MCF-7/HER18 cells and then analyzed the ErbB-2 expression in nuclear and cytoplasmic fractions by immunoblotting. As shown in Fig. 1E, the importin β1 protein level was specifically down-regulated, and ErbB-2 expression in the nuclear fraction was clearly reduced in cells transfected with

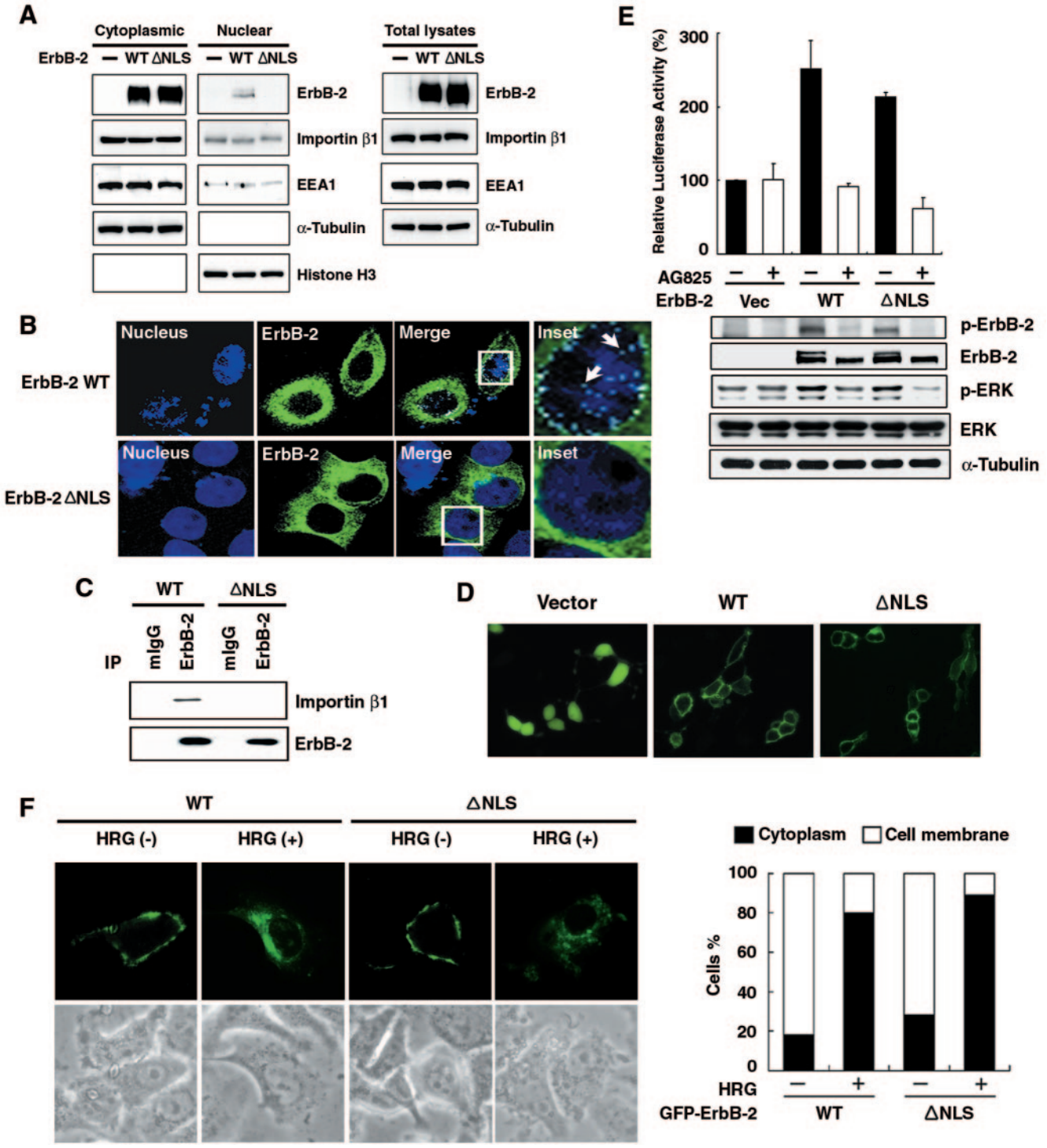

FIG. 2. ErbB-2 mutant with deletion of nuclear localization signal is deficient in nuclear transport. (A) 293 cells were transfected with GFP-tagged wild-type ErbB-2 (WT), GFP-tagged ErbB-2 mutant containing a deficient nuclear localization signal (ΔNLS), or vector control (−). Proteins from the cytoplasmic fraction, nuclear fraction, and total cell lysates were then analyzed by Western blotting with antibodies as indicated. (B) MCF-7 cells were transfected with either GFP-tagged WT or GFP-tagged ΔNLS mutant ErbB-2, and the localization of the ErbB-2 proteins was shown by confocal microscopy. ErbB-2 expression in the nucleus was recognized as white granules (arrows). (C) Lysates from CHO cells transfected with either WT or mutant ΔNLS ErbB-2 constructs were immunoprecipitated (IP) using anti-ErbB-2 or mouse IgG (mIgG) antibodies, and the amount of associated importin β1 was determined by immunoblotting analysis. (D) 293 cells were transfected with the GFP-tagged WT ErbB-2, the GFP-tagged ΔNLS ErbB-2 mutant, or vector control and analyzed by fluorescence microscopy. (E) The GFP-tagged WT or ΔNLS ErbB-2 mutant or vector control (Vec) was cotransfected into cells with the Elk1 fusion transactivator plasmid and luciferase reporter plasmid. After 24 h, the cells were treated with (+) or without (−) tyrosine kinase inhibitor AG825 (80 μM) for 6 h. The luciferase activity induced by the vector alone without AG825 treatment was set as 100%, and the relative luciferase activities are presented as the means with standard deviations of three independent experiments performed in triplicate. Expression of ErbB-2, phosphorylated ErbB-2 (p-ErbB-2), total extracellular signal-

importin β1 siRNA but not in mock-treated cells or cells transfected with nonspecific siRNA. Taken together, these data suggest that importin β1 is required for ErbB-2 translocation into the nucleus.

Mutation of putative NLS blocks ErbB-2 interaction with importin β1 and nuclear localization. NLS is known to contain a stretch of three to five basic residues that is required for nuclear translocation and interaction with importin β1. Analysis of the ErbB-2 sequence using an updated database from the Columbia University Bioinformatics Center detected a cluster of polybasic sequence adjacent to the transmembrane domain. This putative NLS sequence (aa 676-KRRQQKIRK YTMRR-689) is conserved among EGFR family members. To investigate whether this sequence plays a role in ErbB-2 nuclear translocation, a mutant (ErbB-2ΔNLS) was generated by deleting the putative NLS sequence, resulting in the sequence of KLM at the deletion junction, and the cellular extracts of both nuclear and cytoplasmic fractions from WT- and mutant ErbB-2-transfected cells were analyzed by immunoblotting. ErbB-2 expression in the cytoplasm and nucleus was readily visible in the WT ErbB-2-transfected cells. Interestingly, in the ErbB-2ΔNLS-transfected cells, ErbB-2 expression in the nucleus was barely visible but its expression was readily detectable in the cytoplasm (Fig. 2A). This observation was further supported by confocal microscopy, namely, cells transfected with the ErbB-2ΔNLS mutant had barely detectable ErbB-2 in the nucleus (Fig. 2B). Furthermore, IP-WB experiments showed that the ErbB-2ΔNLS mutant was unable to associate with importin β1 (Fig. 2C), indicating that the NLS sequence of ErbB-2 is required for importin β1 binding and nuclear localization. Consistently, the ErbB-2ΔNLS mutant has recently been shown to lose its transactivational activity in the *COX-2* promoter, with which the WT ErbB-2 can interact (49). Despite its defect in nuclear import (Fig. 2A and 2B) and transactivation of genomic target (49), the ErbB-2ΔNLS mutant retains its cell surface location (Fig. 2D) and its ability to transduce the traditional ErbB-2–mitogen-activated protein kinase pathway and to activate the Elk1 target promoter (Fig. 2E) (39). This signaling cascade activated by the ErbB-2ΔNLS mutant or WT ErbB-2 also could be blocked by the ErbB-2-specific tyrosine kinase inhibitor AG825 (reviewed in reference 26) (Fig. 2E). In addition, when WT or ΔNLS ErbB-2 was transfected into SKBr3 cells, treatment with heregulin (1, 18) reduced the level of ErbB-2 in the cell membrane and enhanced ErbB-2 cytoplasmic localization, suggesting that the ErbB-2ΔNLS mutant still undergoes normal internalization (Fig. 2F). Taken together, these results indicate that ErbB-2ΔNLS still possesses the traditional ErbB-2 membrane signaling pathway but, however, loses its ability to interact with importin β1 and becomes unable to translocate into the nucleus.

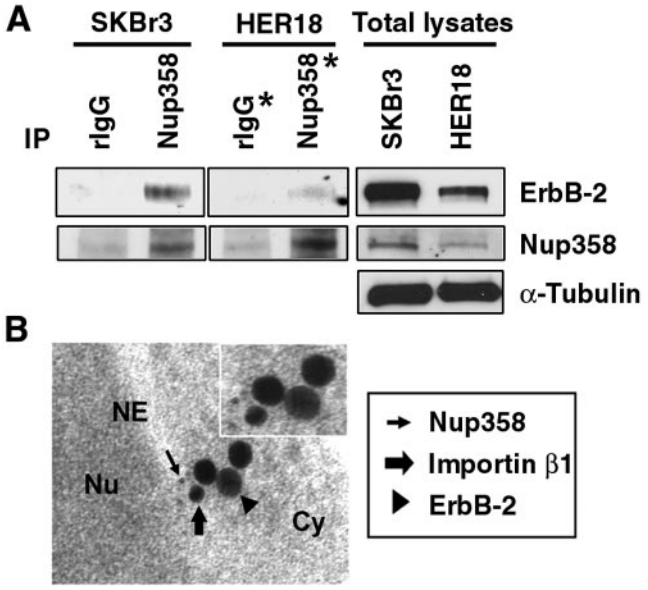

FIG. 3. Interaction between ErbB-2 and nuclear pore protein Nup358. (A) Cell extracts from SKBr3 and MCF-7/HER18 cells were immunoprecipitated (IP) with antibodies against Nup358 and control rIgG, respectively. The immunocomplexes were then analyzed by Western blotting with anti-ErbB-2 (top) and anti-Nup358 (middle) antibodies. Total cell lysates were also analyzed by Western blotting with anti-ErbB-2 (top), anti-Nup358 (middle), and anti-α-tubulin (bottom) antibodies as positive controls. The two lanes marked with asterisks were exposed for a longer period. (B) Immunogold staining of ultrathin sections demonstrated the tricomplex accumulation of Nup358, ErbB-2, and importin β1 at the cytoplasm (Cy) adjacent to the nuclear envelope (NE). An ultrathin section of MDA-MB-453 cells was immunostained for Nup358 (5-nm gold particles, thin arrow), ErbB-2 (30-nm gold particles, arrowhead), and importin β1 (18-nm gold particles, thick arrow). Nu, nucleus.

ErbB-2 interacts with nuclear pore protein Nup358. It has been reported that interaction between importin β1 and nuclear pore protein Nup358, a nucleoporin located at the cytoplasmic filaments of the nuclear pore complexes (NPC) (53, 56), plays a pivotal role in protein nuclear import (2). Since importin β1 association with ErbB-2 is involved in nuclear import of ErbB-2 (Fig. 1), we asked whether Nup358 might associate with ErbB-2 in vivo and be involved in ErbB-2 nuclear translocation. To address this, cell extracts prepared from SKBr3 or MCF-7/HER18 cells were separately subjected to immunoprecipitation with anti-Nup358 antibody or control rIgG antibody and the resulting immunocomplexes were analyzed subsequently by Western blotting with anti-ErbB-2 (Fig. 3A, top) and anti-Nup358 (Fig. 3A, middle) antibodies. As shown in Fig. 3A, ErbB-2 could be coprecipitated using anti-Nup358 antibody, indicating that ErbB-2 interacts with

regulated kinase (ERK), phosphorylated ERK (p-ERK), and α-tubulin proteins was analyzed by Western blotting. (F) SKBr3 cells were transfected with the GFP-tagged WT ErbB-2 or the GFP-tagged ΔNLS ErbB-2 mutant. Twenty-four hours after transfection, the cells were treated with (+) or without (−) heregulin (HRG) (6 ng/ml) for 4 days and analyzed by fluorescence microscopy. The bar diagram indicates the increase of ErbB-2 (GFP) fluorescence in the cytoplasm after cells were treated with heregulin, calculated for a total of 100 cells. The cytoplasm-positive cells were defined as ErbB-2 (GFP) negative in the cell membrane but positive in the cytoplasm. As long as ErbB-2 was detected in a cell membrane, the cell was considered membrane positive regardless of the cytoplasmic status of ErbB-2.

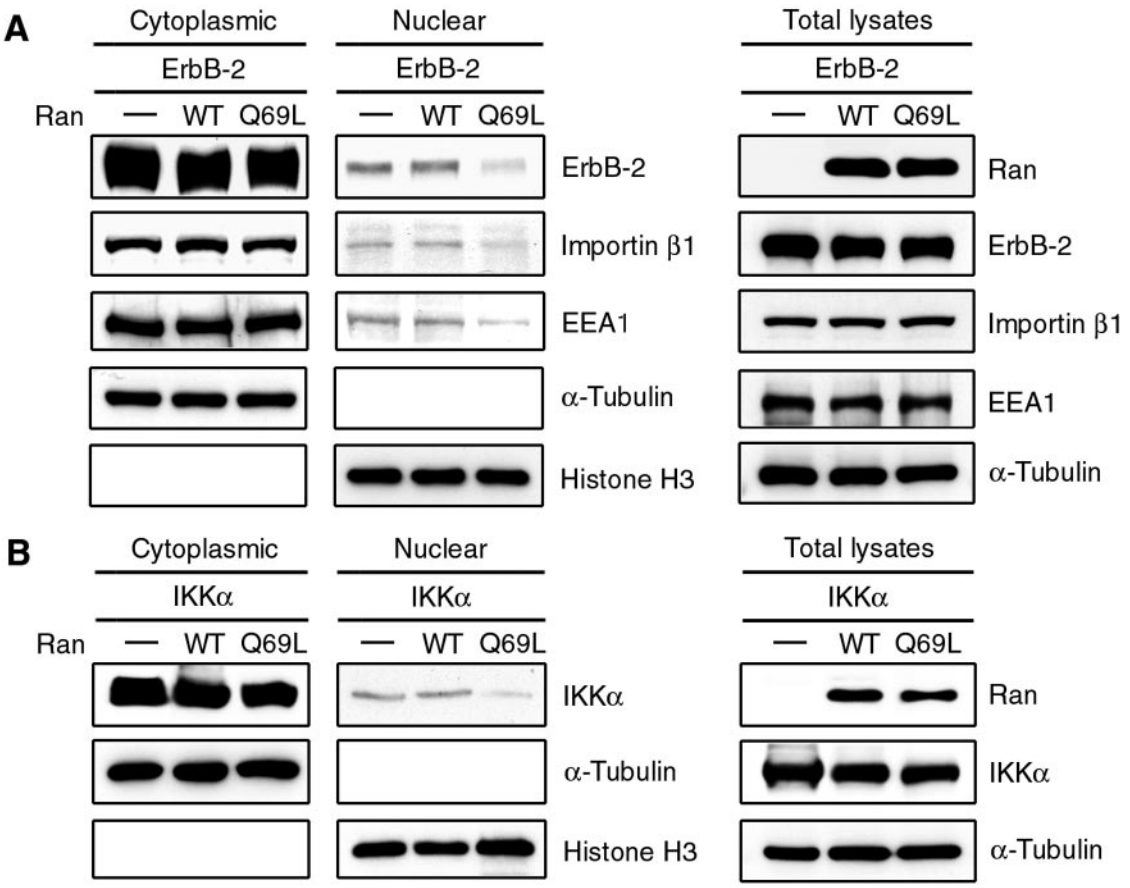

FIG. 4. RanQ69L, a dominant-negative mutant of small GTPase Ran, inhibits the nuclear import of ErbB-2. The Flag-tagged WT Ran, RanQ69L mutant, or vector control (−) was cotransfected into 293 cells with the GFP-tagged WT ErbB-2 (A) or Flag-tagged Ikkα (B) as a positive control. Proteins from the cytoplasmic fraction, the nuclear fraction, and total cell lysates were then analyzed by Western blotting with antibodies as indicated.

Nup358 in vivo. These results were further supported by electron microscopy studies. The gold particles labeling Nup358 (5 nm), ErbB-2 (30 nm), and importin β1 (18 nm) were detectable when the specific primary antibodies against Nup358, ErbB-2, and importin β1 were treated (Fig. 3B). Without treatment of specific primary antibodies, gold particles were not detected even in the presence of gold particle-labeled secondary antibodies (data not shown), indicating the specificity of the detected gold particles. Thus, ErbB-2, Nup358, and importin β1 colocalize at the cytoplasm close to the nuclear envelope. These data suggest that Nup358, like importin β1, may be involved in nuclear translocation of ErbB-2, implying that ErbB-2 may traverse the nuclear pore via interaction with importin β1 and nuclear pore protein Nup358, resulting in nuclear translocation.

Inhibition of ErbB-2 nuclear import by RanQ69L, a dominant-negative mutant of small GTPase Ran. It is well documented that the nucleotide-bound state of small GTPase Ran plays a key role in nuclear transport. As the importin-NLS-cargo complex translocates into the nucleus, the cargo is released from importin into the nucleoplasm by binding of RanGTP to importin β1 (reviewed in reference 50). The asymmetric distribution of RanGTP and RanGDP is therefore critical for transport in and out of the nucleus. Most nuclear Ran is presented in the GTP-bound form, while cytoplasmic Ran is predominantly in the GDP-bound form. Experimental perturbation of the RanGDP-RanGTP gradient blocks the nuclear transport. A dominant-negative mutant of Ran (RanQ69L) deficient in GTPase activity prevents nuclear import of the protein (reviewed in reference 30). Thus, we investigated the effect of RanQ69L on the nuclear localization of ErbB-2 by cellular fractionation and immunoblotting analysis. Using Ikkα (22) as a positive control (Fig. 4B), the ErbB-2 expression in the nucleus was significantly reduced in cells cotransfected with RanQ69L but not in cells cotransfected with WT Ran or vector control (Fig. 4A), suggesting the involvement of Ran in the nuclear import of ErbB-2. Consistently, RanQ69L also reduced the nuclear localization of importin β1. These results indicate that the activity of Ran is required for ErbB-2 nuclear transport.

Inactivation of nuclear export receptor leads to accumulation of ErbB-2 in the nucleus. Proteins exported from the nucleus are recognized by exportins, the export receptors (reviewed in references 15 and 33), and the inhibition of nuclear export leads to nuclear elevation of proteins. Since ErbB-2 may use importin β1/Nup358 as a transport carrier to translocate to the nucleus, we asked whether it can also be exported through the well-characterized exportin Crm1 (25). To this end, we

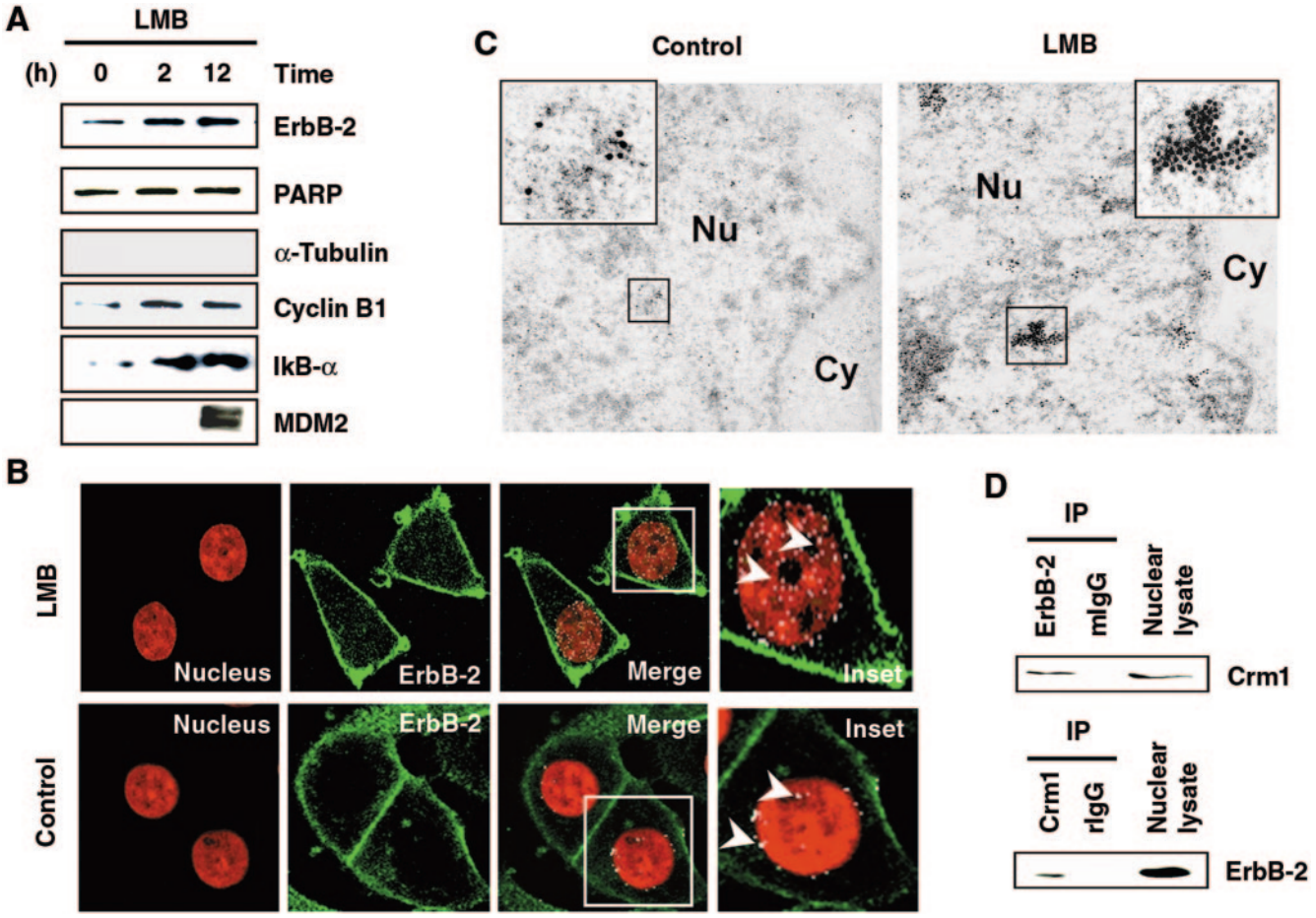

FIG. 5. Inactivation of nuclear export receptor leads to accumulation of ErbB-2 in the nucleus. (A) Nuclear extracts from MCF-7/HER18 cells treated with 20-ng/ml LMB for the indicated times were analyzed for nuclear ErbB-2 by Western blot analysis using anti-ErbB-2 antibody. Similarly, aliquots of the nuclear extracts were also analyzed by Western blot analysis using indicated antibodies as positive controls. Absence of α-tubulin in the nucleus indicates that there is no cytoplasmic contamination in the nuclear extract. (B) MCF-7/HER18 cells were treated with 20-ng/ml LMB for 12 h and stained for ErbB-2 by immunofluorescence analysis and examined under a confocal laser microscope. ErbB-2 localization in the nucleus was recognized as white granules (arrowheads). (C) Immunogold staining of ultrathin sections for ErbB-2 showed the accumulation of ErbB-2 in the nucleus of control (left panel, inset) and in the nucleus of LMB-treated MCF-7/HER18 cells (right panel, inset). The gold particles labeled ErbB-2 (15 nm). Cy, cytoplasm; Nu, nucleus. (D) Nuclear lysates from MCF-7/HER18 cells were immunoprecipitated (IP) using mouse anti-ErbB-2 antibody or mouse IgG (mIgG) antibody and Western blotted with anti-Crm1 antibody (upper panel). Similarly, equal amounts of lysate were also used for reciprocal immunoprecipitation using rabbit anti-Crm1 antibody or rIgG antibody and blotted with anti-ErbB-2 antibody (lower panel).

treated cells with leptomycin B (LMB), which inactivates Crm1, thus inhibiting the nuclear export of proteins. Treatment with LMB resulted in accumulation of ErbB-2 in the nucleus by 2 h (Fig. 5A), and the level was still maintained by 12 h. As a positive control, nuclear lysates from LMB-treated cells revealed elevated levels of other molecules, such as IκBα, cyclin B1, and MDM2, known to be arrested by such treatment (14, 19, 55). Nuclear retention of ErbB-2 resulting from LMB treatment was also supported by localization studies using a confocal microscope. ErbB-2 in the nucleus was elevated following this treatment (Fig. 5B, arrowheads). There is more ErbB-2 in the nucleus of the LMB-treated cells than in that of the untreated cells. In addition, electron microscopy studies support the nuclear retention of ErbB-2 resulting from LMB treatment (Fig. 5C). To further confirm the involvement of Crm1 in ErbB-2 nuclear export, the molecular interaction between ErbB-2 and Crm1 was examined using IP-WB analysis. Precipitates of anti-ErbB-2 or anti-Crm1 antibodies demonstrated interaction between Crm1 and ErbB-2 in the nuclear extracts (Fig. 5D). This interaction was specific, as the complex was not detectable by the normal immunoglobulins. As ErbB-2 is provided with its nuclear entry by importin, ErbB-2–Crm1 complex formation and the intranuclear elevation following LMB treatment support the idea of Crm1-mediated nuclear export of ErbB-2.

Possible involvement of clathrin-mediated endocytic internalization in nuclear translocation of cell membrane ErbB-2. The results described above indicate that ErbB-2, similar to many nucleocytoplasmic shuttling proteins, interacts with importin β1, Crm1, and an NPC protein, Nup358, suggesting that ErbB-2 may also shuttle between the nucleus and the cytoplasm with the involvement of NPC. However, it is still virtually unknown how cell surface ErbB-2 receptor may be translocated to the nucleus through the cytoplasm. One of the

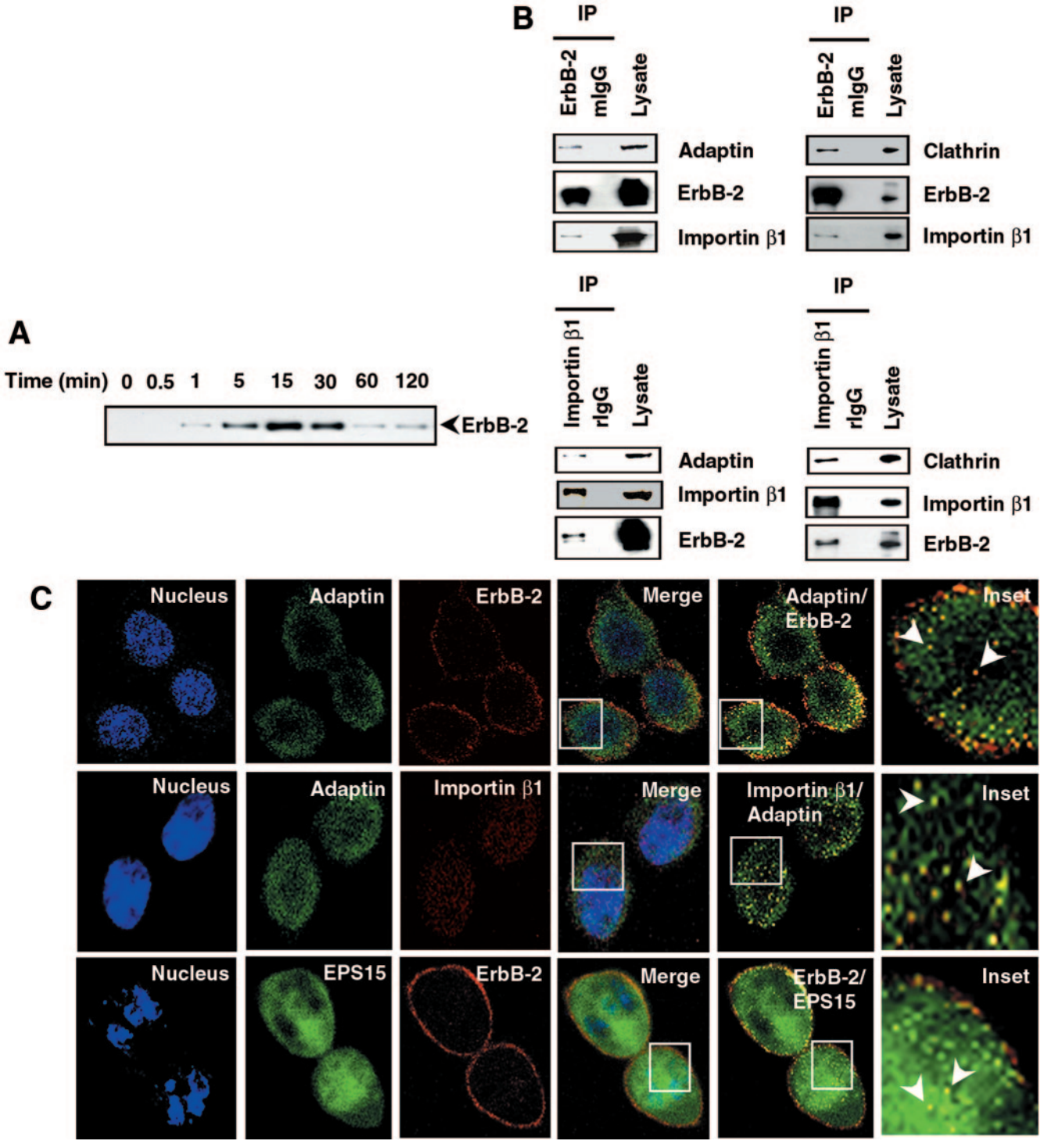

FIG. 6. Involvement of clathrin-mediated endocytic internalization in nuclear translocation of cell membrane ErbB-2. (A) MCF-7/HER18 cells were biotinylated at 4°C using normal human serum-biotin. The biotinylated molecules on the cell surface were released to internalize by incubation at 37°C for the indicated times. Nuclear extracts were then affinity purified with avidin-conjugated agarose and analyzed by Western blotting with anti-ErbB-2 antibody. (B) Cell lysates from MCF-7/HER18 cells were immunoprecipitated (IP) with anti-ErbB-2, anti-importin β1, mouse IgG (mIgG), or rIgG. The precipitated immunocomplexes were then analyzed by Western blotting with adaptin, clathrin, importin β1, and ErbB-2. (C) Immunofluorescence staining of ErbB-2, importin β1, and the endocytosis proteins adaptin and EPS15 visualized them under confocal microscopy. Top and middle panels: endogenous adaptin (green) and ErbB-2 (red) (top panels) and adaptin (green) and importin β1 (red) (middle panels) colocalized in MCF-7/HER18 cells. Bottom panels: GFP-EPS15 expression vectors were cotransfected with ErbB-2 into CHO cells. The cells were then immunostained for ErbB-2 (red) and studied by confocal microscopy. Arrowheads in the insets indicate nuclear colocalization.

difficulties in appreciating nuclear translocalization of cell surface tyrosine kinase receptors is posed by the question of how the membrane-bound tyrosine kinase receptors overcome the energy barrier and travel to the nucleus through the cytoplasm. One way to allow membrane-bound receptors to enter the cytoplasm is through endocytosis, a complex process of receptor internalization (reviewed in reference 11). Following endocytosis, the vesicles harboring the receptors translocate intracellularly. To address whether endocytosis may be involved in nuclear translocation of cell surface ErbB-2, we first verified that cell surface ErbB-2 can translocate to the nucleus and then asked whether endocytic internalization of ErbB-2 may play a role in nuclear immigration. The cell surface ErbB-2 was labeled via biotinylation (31), a process that labels only cell surface molecules, and the nuclear extracts from these cells were analyzed for the biotinylated ErbB-2 to detect nuclear translocation of cell surface ErbB-2. Affinity purification using avidin followed by Western blot analysis demonstrated ErbB-2 in the nuclear extracts within 1 min, and ErbB-2 then reached peak level around 15 to 30 min. It is interesting that the level of biotinylated nuclear ErbB-2 significantly dropped within 60 min (Fig. 6A). Similar results were obtained when another cell line, MDA-MB-453, was analyzed (data not shown). These data, together with ErbB-2–Crm1 interaction data (Fig. 5D), suggest that cell surface receptor ErbB-2 translocates to the nucleus and that the nuclear ErbB-2 may then be exported by Crm1-mediated nuclear export within 1 h. Next we asked whether this entry is mediated through endocytosis. To address this issue, we carried out a series of IP-WB assays using an anti-ErbB-2 antibody to IP cell lysates and the precipitates were studied for the detection of the molecules involved in endocytosis, such as adaptin and clathrin (reviewed in reference 11). Typically, clathrins assemble to deform the cell membrane into coated pits, adaptin interacts directly with internalization motifs in the cargo, EPS15 regulates coat assembly through constitutive binding to the AP2 complex, and dynamin plays a pivotal role in vesicle fission. These molecules orchestrate themselves, leading to the fission of endocytic vesicles known as endosomes. Complexes pulled down by ErbB-2 antibody contained both adaptin and clathrin (Fig. 6B, upper panel). Interestingly, analysis of the precipitates also detected importin β1, suggesting its affiliation with the complexes. Similar studies using anti-importin β1 antibody also pulled down complexes containing adaptin and clathrin besides ErbB-2 (Fig. 6B, lower panel). In addition, proteins such as EPS15 and dynamin 2 were also detected in the complexes pulled down by ErbB-2 or importin β1 (see Fig. S1 in the supplemental material). These data suggest that importin β1 and ErbB-2 form complexes with multiple accessory endocytic proteins. Biochemical evidence of ErbB-2 interaction with the endocytosis markers was further provided by confocal analysis. ErbB-2 colocalized with adaptin (Fig. 6C, top panel) and EPS15 (Fig. 6C, bottom panel), and adaptin colocalized with importin β1 (Fig. 6C, middle panel). The confocal analyses were carried out by using antibody against endogenous adaptin or the cotransfection method using GFP-tagged EPS15 (3) plasmid and ErbB-2 construct. Taken together, these data indicate that ErbB2, similar to other RTKs, forms complexes with endocytosis accessory proteins and that, importantly, importin β1 is also involved in the complexes.

Nuclear translocation of ErbB-2 by endosomal sorting. We next asked whether the endocytic vesicles that eventually yield endosomes also form a complex with importin β1 and ErbB-2. If so, a model depicted in Fig. 7A will provide a plausible mechanism for nuclear translocation of cell surface RTKs: the endosome can serve as a vehicle to carry the cell surface tyrosine kinase receptors, and importin β1 can interact with the nuclear localization sequence of tyrosine kinase receptors (shown above) and serve as a guide to drive the tyrosine kinase receptor-containing vehicles to the nucleus through interaction with NPC proteins such as Nup358 (Fig. 7A). To test this model, electron microscopy was used to demonstrate the presence of importin β1–ErbB-2 complex in the endosome (Fig. 7B). The electron microscopy data indicate that ErbB-2 and importin β1 can be colocalized in the endosome wall. In addition, colocalization of the endosomal marker EEA1 (early endosome antigen 1) and ErbB-2 both in the cytoplasm and in the nucleus was detected by electron microscopy (Fig. 7C, insets 2 and 3) and confocal immunofluorescence (Fig. 7D). The association between EEA1 and ErbB-2 was further confirmed by an IP-WB experiment using an anti-EEA1 antibody for IP (Fig. 7E). The EEA1 was also shown to interact with importin β1. Similar results were obtained when an anti-ErbB-2 antibody was used for IP to carry out the reciprocal IP-WB experiment (data not shown). To further examine whether ErbB-2, EEA1, and importin β1 form a complex, double IP-WB assays were performed using antibodies against ErbB-2 and EEA1 for first and second IPs and then WB with importin β1 antibody. The results support the idea that the three molecules form a trimeric complex (Fig. 7F). It is interesting that the colocalized ErbB-2 and EEA1 cluster at the nucleocytoplasmic juncture of the nuclear envelope (Fig. 7C, inset 1). Colocalization of ErbB-2 and EEA1 was also detectable in the nucleus and cytoplasm (data not shown) and at the nucleocytoplasmic juncture of the nuclear envelope in another breast cancer cell line, MDA-MB-453 (see Fig. S2A in the supplemental material). Results of electron microscopy also demonstrated that ErbB-2 and importin β1 formed a colocalized cluster at the nuclear envelope (see Fig. S2B, inset 1, in the supplemental material), as well as demonstrating localization of ErbB-2 in the nucleus (see Fig. S2B, inset 2, in the supplemental material) and the cytoplasm (data not shown and Fig. 1D). Thus, these results indicated that ErbB-2, importin β1, and endosomal proteins form complexes in the cytoplasm and the nucleus, a conclusion derived based on multiple experimental methods, including immunoprecipitation, confocal immunofluorescence, and immunoelectron microscopy. In addition, knocking down importin β1 by siRNA or inactivation of small GTPase Ran by RanQ69L abrogated nuclear transport of ErbB-2 as mentioned above and also alleviated the expression of EEA1 in the nucleus as shown by cellular fractionation and immunoblotting analysis (Fig. 1E and 4A). Together, the results strongly support the idea that nuclear transport of ErbB-2 by importin β1 involves endosomal sorting (Fig. 7A).

Endocytosis is required for ErbB-2 nuclear translocation. The involvement of endosomal sorting in ErbB-2 nuclear transport predicts that inhibition of endocytosis can block this process. To test this hypothesis, endocytosis was inhibited by using a dominant-negative mutant dynamin, which contains a point mutation (K44A) in the GTPase domain. This mutation

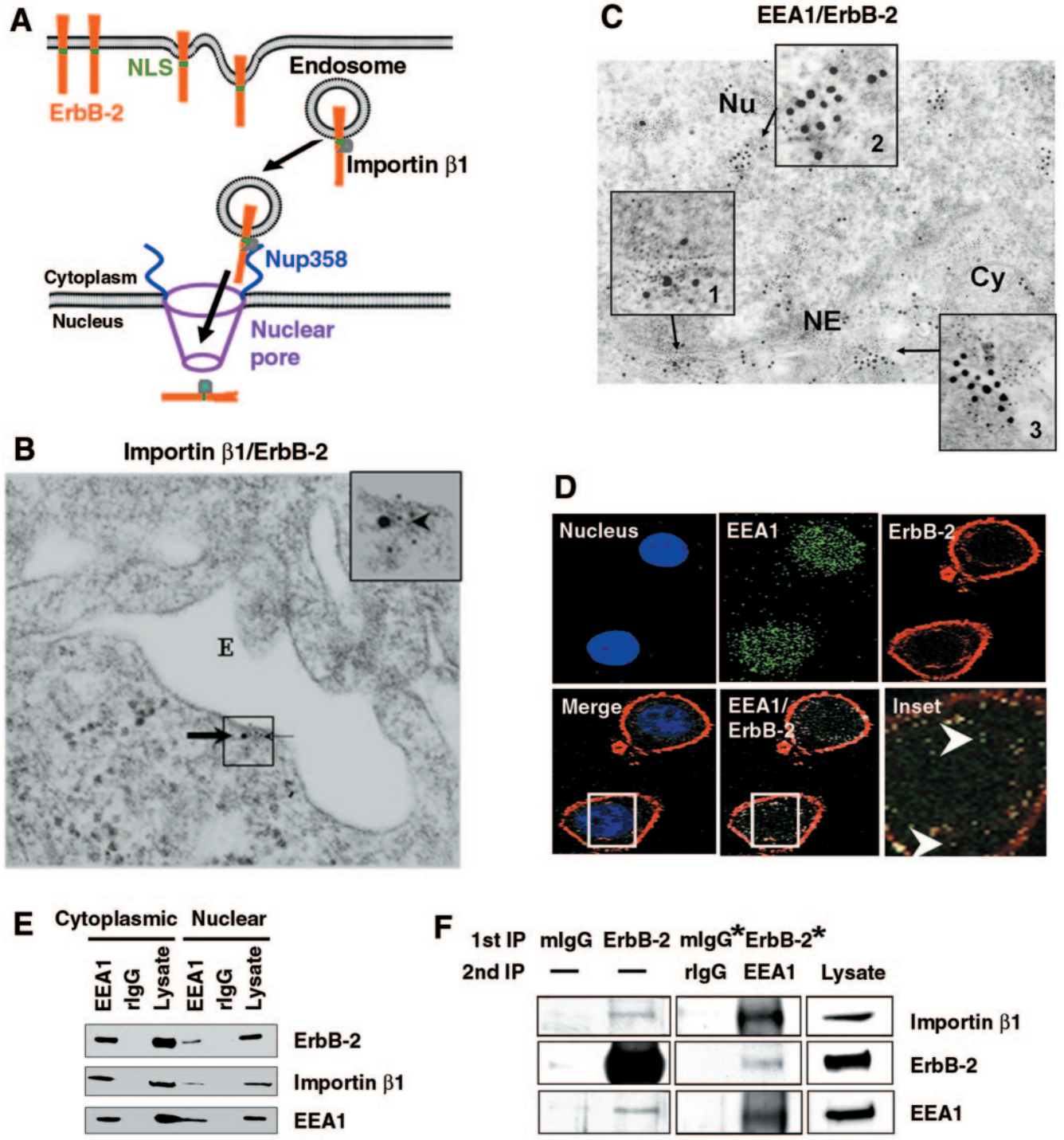

FIG. 7. Nuclear translocation of ErbB-2 by endosomal sorting. (A) Model for importin β1-mediated ErbB-2 nuclear transport by endosomal sorting. The scale of the diagram does not reflect the relative sizes of different molecules and the subcellular structures. (B) ErbB-2 and importin β1 colocalized in the endosome wall by electron microscopy. An ultrathin section of MCF-7/HER18 cells was immunostained for ErbB-2 (15-nm gold particles, thick arrow) and importin β1 (5-nm gold particles, thin arrow). The arrowhead indicates colocalization of the two proteins in the endosome (E) wall. (C) ErbB-2 and EEA1 colocalization in the cytoplasm and nucleus was demonstrated by electron microscopy. Ultrathin sections from MCF-7/HER18 cells were immunostained for ErbB-2 (5-nm gold particles) and EEA1 (15-nm gold particles). Inset 1 reveals the colocalization of ErbB-2 and EEA1 at the nuclear envelope (NE); inset 2 shows the colocalization of ErbB-2 and EEA1 in the nucleus (Nu); inset 3 indicates the colocalization of ErbB-2 and EEA1 in the cytoplasm (Cy). An arrow indicates the source of the inset. (D) MCF-7/HER18 cells were immunostained for EEA1 (green) and ErbB-2 (red) and analyzed by confocal microscopy. Colocalization of EEA1 and ErbB-2 in the nucleus (arrowhead) is indicated in the inset panel. (E) Cytoplasmic and nuclear lysates from MCF-7/HER18 cells were immunoprecipitated with rabbit anti-EEA1 antibody or control rIgG antibody. The immunocomplexes were then analyzed by Western blotting with indicated antibodies. (F) ErbB-2 and importin β1 form complexes with endosomal protein EEA1. Cell extracts from MCF-7/HER18 cells were first immunoprecipitated (1st IP) with antibodies against ErbB-2 or control mouse IgG (mIgG), followed by a second immunoprecipitation (2nd IP) with antibodies against EEA1 or control rIgG. The immunocomplexes were subjected to Western blotting with anti-importin β1 (top), anti-ErbB-2 (middle), and anti-EEA1 (bottom) antibodies. Total cell lysate and single immunoprecipitation with anti-ErbB-2 or mouse IgG antibodies were used as positive controls. The minus sign indicates the absence of antibody. The two lanes marked with asterisks were exposed for a longer period.

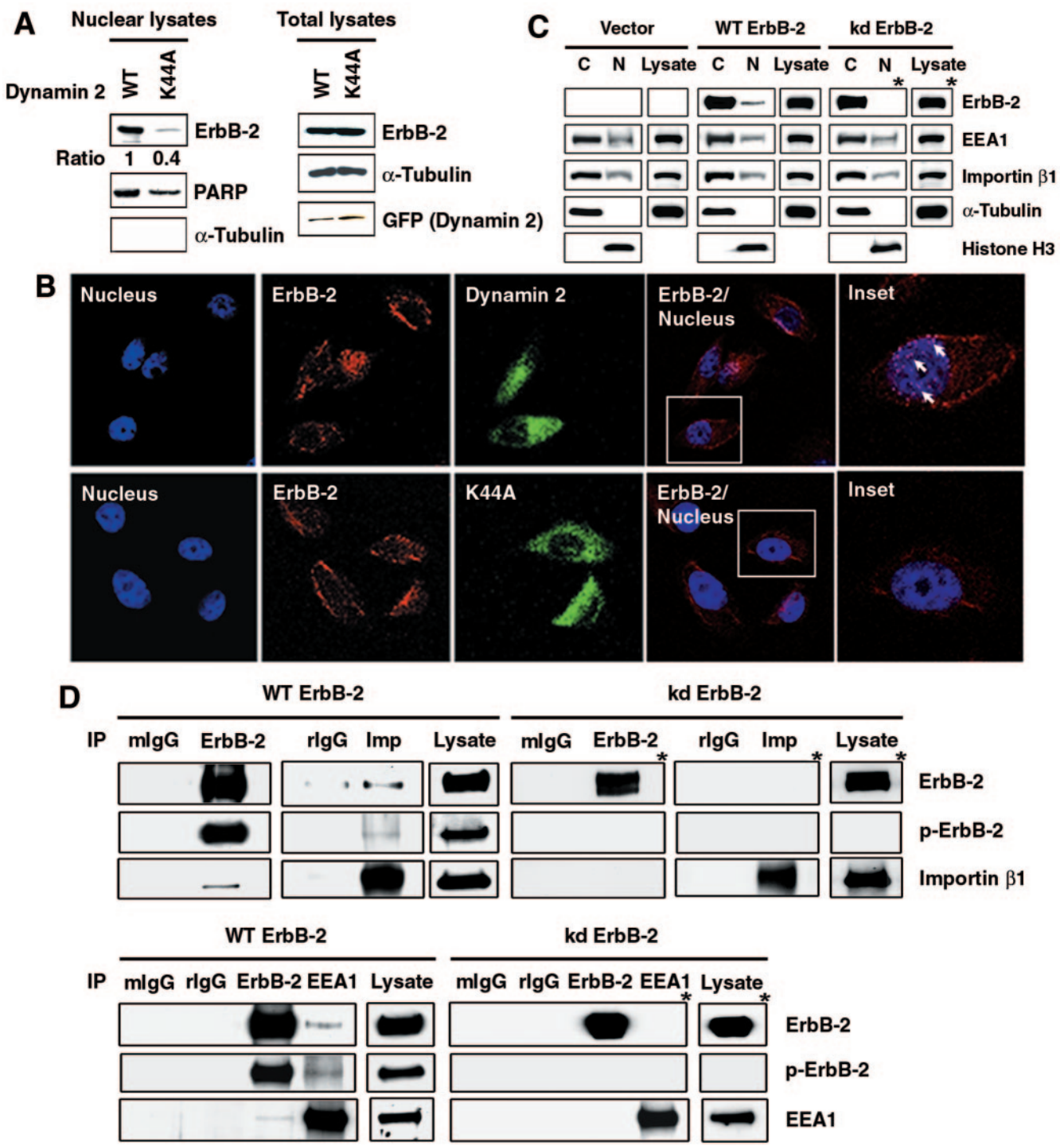

FIG. 8. ErbB-2 nuclear translocation requires endocytosis. (A) Dynamin activity is required for nuclear localization of ErbB-2. CHO cells were transfected with ErbB-2 cDNA together with GFP-tagged WT or GFP-tagged K44A mutant (K44A) dynamin 2 cDNA. Left panels: the nuclear lysates from these cells were analyzed by Western blotting using antibodies against ErbB-2, PARP, and α-tubulin. The levels of ErbB-2 expression were quantitated and normalized to the protein levels of PARP. The expression level of ErbB-2 in GFP-tagged WT dynamin 2-transfected cells was set as 1. Right panels: total cell lysates were blotted for equal expression of ErbB-2, α-tubulin, and dynamin 2 (GFP). (B) CHO cells were transfected with the GFP-tagged WT (top) or K44A mutant (bottom) dynamin 2 together with ErbB-2 plasmid. Localization of ErbB-2 (red) in the TOPRO 3-stained nucleus (blue) was examined under a confocal microscope. ErbB-2 localized in the nucleus is shown in pink spots as indicated by arrows in the inset. (C) Cytoplasmic fractions (C), nuclear fractions (N), and total cell lysates from MCF-7/WT ErbB-2, MCF-7/kinase-deficient mutant ErbB-2 (kd ErbB-2), or vector control cells were analyzed by Western blotting with antibodies as indicated. (D) Lysates from MCF-7/WT ErbB-2 and MCF-7/kd ErbB-2 cells were immunoprecipitated (IP) with ErbB-2, importin β1 (Imp), EEA1, control mouse IgG (mIgG), and rIgG. The immunocomplexes were then analyzed by Western blotting with antibodies as indicated. Total cell lysates were also analyzed by Western blotting with anti-ErbB-2, antiphosphotyrosine (p-ErbB-2), anti-importin β1, and anti-EEA1 antibodies as positive controls. The blots marked with asterisks were exposed for a longer period.

abrogates dynamin enzymatic activity and inhibits separation of the coated pit from the plasma membrane (6; reviewed in reference 42). Expression of the K44A dynamin mutant blocked nuclear expression of ErbB-2 as shown by WB (Fig. 8A), which was also supported by immunofluorescence staining (Fig. 8B), in which cotransfection of the GFP-tagged K44A mutant dynamin and ErbB-2 resulted in decreased nuclear expression of ErbB-2 compared with the WT dynamin-transfected cells (Fig. 8B, arrows). Tyrosine kinase activity of RTKs is also known to be required for endocytosis, so we examined the nuclear expression of the kinase-deficient mutant ErbB-2 (kd ErbB-2) by cellular fractionation and immunoblotting analysis. ErbB-2 protein was readily detected in the cytoplasm and nucleus in the WT ErbB-2-transfected cells. However, in the kd ErbB-2-transfected cells, ErbB-2 expression was disrupted in the nucleus but was readily detectable in the cytoplasm (Fig. 8C). Moreover, IP-WB experiments showed that the kd ErbB-2 mutant was unable to associate with importin β1 (Fig. 8D, upper panels) and EEA1 (Fig. 8D, lower panels), supporting the notion that kd ErbB-2, defective in endocytosis, was unable to translocate into the nucleus. Taken together, these results indicate that endocytic internalization is required for nuclear transport of ErbB-2 and thus support the model shown in Fig. 7A.

DISCUSSION

Our proposed model (Fig. 7A) hypothesizes the following: during endocytic internalization or endosomal sorting, ErbB-2 and importin β1 can interact with each other and travel together with other endocytic adaptor proteins and, finally, translocate into the nucleus via binding to nuclear pore protein. This mode of transport is novel and clearly indicates that endocytosis is required for nuclear localization.

Consistent with this notion, nuclear translocation of RTKs and their transcriptional function can be blocked by tyrosine kinase inhibitors (27, 49) and tyrosine kinase activity is known to be required for endocytosis. Indeed, the kd ErbB-2 mutant was unable to translocate into the nucleus (Fig. 8C). It is worth mentioning that heregulin (gp30) localizes ErbB-2 perinuclearly with a mechanism potentially involved with heregulin-mediated ErbB-2 translocation (1). In addition, the nucleocytoplasmic shuttling of endocytic proteins is believed to play a role in transcription (48), but how these bona fide proteins of endocytosis enter the nucleus is unknown. The proposed model also provides a mode for their transport to the nucleus.

It should be mentioned that our current data show that the nuclear localization of the endocytic protein EEA1 did not change in cells expressing ErbB-2 ΔNLS or kd ErbB-2 mutants compared with the vector control cells and cells expressing WT ErbB-2 (Fig. 2A and 8C). However, under conditions of nuclear import being blocked by siRNA knockdown of importin β1 (Fig. 1E) or mutant RanQ69L (Fig. 4A), we did observe inhibition of nuclear translocation of ErbB-2 and EEA1. This is likely due to a possibility that ErbB-2 is not the only membrane protein translocating into the nucleus through endosomal sorting; other receptor tyrosine kinases in the membrane may enter the nucleus through similar mechanisms. Blockage of the nuclear translocation process by importin β1 downregulation or treatment of mutant RanQ69L may have a general effect of inhibiting the nuclear translocation of many membrane receptors that interact with EEA1; therefore, EEA1 expression in the nucleus is inhibited (Fig. 1E and 4A). In the case of ErbB-2 ΔNLS and kd ErbB-2 mutants, the nuclear expression of EEA1 will not be significantly changed (Fig. 2A and 8C), as EEA1 still interacts with many other receptors to translocate into the nucleus. In addition, it has been reported that endocytic proteins, including EPS15, epsin 1, Eps15R, α-adaptin, and the clathrin assembly lymphoid myeloid leukemia protein, shuttle in and out of the nucleus (10, 12, 20, 48). The nucleocytoplasmic shuttling of endocytic proteins appears to be a constitutive process (48). It is likely that EEA1 may behave similarly to these endocytic proteins. Thus, it is reasonable not to detect the substantial nuclear localization change of endocytic protein EEA1 at steady state in cells expressing the ErbB-2 ΔNLS or kd ErbB-2 mutant.

Endosomes have been recognized as platforms for the continuation of signaling emanating from the plasma membrane. Endosomal sorting of membrane ErbB-2 to the nucleus is an example of emerging compartmentalized signaling with immense biological implications. Supporting this is the recently described ras signaling from different membrane compartments of the endoplasmic reticulum and Golgi complex (9) which is no longer limited to the plasma membrane, as it continues on the endomembrane. In addition, Bild et al. also indicated that, following growth factor stimulation, STAT3 translocates from the cell membrane to the perinuclear region via endocytic vesicles, and this translocation is essential for STAT3-dependent gene regulation (5), supporting the notion that endocytic vesicles may function as a vehicle to carry cargo proteins for nuclear translocation. Thus, the novel finding described herein delineates the transport mechanism that carries ErbB-2 to the nucleus as an intact molecule and may explain the missing link between signaling of membrane ErbB-2 and its nuclear function. What still remains a puzzle is how ErbB-2 embedded in the membrane of the endosome can pass through the nuclear envelope and enter the nucleus. The interaction between ErbB-2 and Nup358 suggests the involvement of NPC. However, more systemic studies are required to clearly define the detailed mechanism. In spite of extensive studies on nucleocytoplasmic shuttling for a large number of cellular proteins (14, 19, 55; reviewed in reference 47) and elegant work on the structure of NPC, the specific mechanism for how a cellular protein travels through the NPC still remains unsolved (reviewed in reference 47). The current model (Fig. 7A) adds the new complication of how the lipid bilayer of the endosome is removed when the ErbB-2/importin β1 and EEA1 complex travel through the nuclear envelope. Nevertheless, the model provides a logical route for ErbB-2 nuclear translocation from the cell surface and may serve as a general mechanism for other RTKs or cell surface receptors and thus show a new avenue for understanding interactions between the cell surface and the nucleus.

ACKNOWLEDGMENTS

We thank Karsten Weis, Mark A. McNiven, and Alexandre Benmerah for their generosity in providing pQE-Ran, pQE-RanQ69L, GFP-tagged dynamin 2, GFP-tagged K44A dynamin 2, and GFP-tagged EPS15.

This work was supported by grants from NIH, RO1 CA109311 and PO1 CA099031, and The National Breast Cancer Research Foundation, Inc. (to M.-C.H.) and by M. D. Anderson Cancer Center supporting grant CA16672.

REFERENCES

1. **Bacus, S. S., E. Huberman, D. Chin, K. Kiguchi, S. Simpson, M. Lippman, and R. Lupu.** 1992. A ligand for the erbB-2 oncogene product (GP30) induces differentiation of human breast cancer cells. Cell Growth Differ. **3:**401–411.
2. **Ben-Efraim, I., and L. Gerace.** 2001. Gradient of increasing affinity of importin beta for nucleoporins along the pathway of nuclear import. J. Cell Biol. **152:**411–417.
3. **Benmerah, A., C. Lamaze, B. Begue, S. L. Schmid, A. Dautry-Varsat, and N. Cerf-Bensussan.** 1998. AP-2/Eps15 interaction is required for receptor-mediated endocytosis. J. Cell Biol. **140:**1055–1062.
4. **Benz, C. C., G. K. Scott, J. C. Sarup, R. M. Johnson, D. Tripathy, E. Coronado, H. M. Shepard, and C. K. Osborne.** 1993. Estrogen-dependent, tamoxifen-resistant tumorigenic growth of MCF-7 cells transfected with HER2/neu. Breast Cancer Res. Treat. **24:**85–95.
5. **Bild, A. H., J. Turkson, and R. Jove.** 2002. Cytoplasmic transport of Stat3 by receptor-mediated endocytosis. EMBO J. **21:**3255–3263.
6. **Cao, H., F. Garcia, and M. A. McNiven.** 1998. Differential distribution of dynamin isoforms in mammalian cells. Mol. Biol. Cell **9:**2595–2609.
7. **Cao, H., H. M. Thompson, E. W. Krueger, and M. A. McNiven.** 2000. Disruption of Golgi structure and function in mammalian cells expressing a mutant dynamin. J. Cell Sci. **113:**1993–2002.
8. **Carpenter, G.** 2003. Nuclear localization and possible functions of receptor tyrosine kinases. Curr. Opin. Cell Biol. **15:**143–148.
9. **Chiu, V. K., T. Bivona, A. Hach, J. B. Sajous, J. Silletti, H. Wiener, R. L. Johnson II, A. D. Cox, and M. R. Philips.** 2002. Ras signaling on the endoplasmic reticulum and the Golgi. Nat. Cell Biol. **4:**343–350.
10. **Coda, L., A. E. Salcini, S. Confalonieri, G. Pelicci, T. Sorkina, A. Sorkin, P. G. Pelicci, and P. P. Di Fiore.** 1998. Eps15R is a tyrosine kinase substrate with characteristics of a docking protein possibly involved in coated pits-mediated internalization. J. Biol. Chem. **273:**3003–3012.
11. **Conner, S. D., and S. L. Schmid.** 2003. Regulated portals of entry into the cell. Nature **422:**37–44.
12. **Doria, M., A. E. Salcini, E. Colombo, T. G. Parslow, P. G. Pelicci, and P. P. Di Fiore.** 1999. The eps15 homology (EH) domain-based interaction between eps15 and hrb connects the molecular machinery of endocytosis to that of nucleocytosolic transport. J. Cell Biol. **147:**1379–1384.
13. **Feng, Y., V. J. Venema, R. C. Venema, N. Tsai, and R. B. Caldwell.** 1999. VEGF induces nuclear translocation of Flk-1/KDR, endothelial nitric oxide synthase, and caveolin-1 in vascular endothelial cells. Biochem. Biophys. Res. Commun. **256:**192–197.
14. **Freedman, D. A., and A. J. Levine.** 1998. Nuclear export is required for degradation of endogenous p53 by MDM2 and human papillomavirus E6. Mol. Cell. Biol. **18:**7288–7293.
15. **Gorlich, D., and U. Kutay.** 1999. Transport between the cell nucleus and the cytoplasm. Annu. Rev. Cell Dev. Biol. **15:**607–660.
16. **Graham, J. M., and D. Rickwood.** 1997. Subcellular fractionation: a practical approach. IRL Press at Oxford University Press, Oxford, United Kingdom.
17. **Hanada, N., H. W. Lo, C. P. Day, Y. Pan, Y. Nakajima, and M. C. Hung.** Co-regulation of B-Myb expression by E2F1 and EGFR receptor. Mol. Carcinog., in press.
18. **Holmes, W. E., M. X. Sliwkowski, R. W. Akita, W. J. Henzel, J. Lee, J. W. Park, D. Yansura, N. Abadi, H. Raab, G. D. Lewis, et al.** 1992. Identification of heregulin, a specific activator of p185erbB2. Science **256:**1205–1210.
19. **Huang, T. T., N. Kudo, M. Yoshida, and S. Miyamoto.** 2000. A nuclear export signal in the N-terminal regulatory domain of IκBα controls cytoplasmic localization of inactive NF-κB/IκBα complexes. Proc. Natl. Acad. Sci. USA **97:**1014–1019.
20. **Hyman, J., H. Chen, P. P. Di Fiore, P. De Camilli, and A. T. Brunger.** 2000. Epsin 1 undergoes nucleocytosolic shuttling and its eps15 interactor NH_2-terminal homology (ENTH) domain, structurally similar to Armadillo and HEAT repeats, interacts with the transcription factor promyelocytic leukemia Zn^{2+} finger protein (PLZF). J. Cell Biol. **149:**537–546.
21. **Ilan, N., A. Tucker, and J. A. Madri.** 2003. Vascular endothelial growth factor expression, beta-catenin tyrosine phosphorylation, and endothelial proliferative behavior: a pathway for transformation? Lab. Investig. **83:**1105–1115.
22. **Jiang, X., N. Takahashi, K. Ando, T. Otsuka, T. Tetsuka, and T. Okamoto.** 2003. NF-κB p65 transactivation domain is involved in the NF-κB-inducing kinase pathway. Biochem. Biophys. Res. Commun. **301:**583–590.
23. **Johnston, C. L., H. C. Cox, J. J. Gomm, and R. C. Coombes.** 1995. Fibroblast growth factor receptors (FGFRs) localize in different cellular compartments. A splice variant of FGFR-3 localizes to the nucleus. J. Biol. Chem. **270:**30643–30650.
24. **Jurata, L. W., S. L. Pfaff, and G. N. Gill.** 1998. The nuclear LIM domain interactor NLI mediates homo- and heterodimerization of LIM domain transcription factors. J. Biol. Chem. **273:**3152–3157.
25. **Kudo, N., N. Matsumori, H. Taoka, D. Fujiwara, E. P. Schreiner, B. Wolff, M. Yoshida, and S. Horinouchi.** 1999. Leptomycin B inactivates CRM1/exportin 1 by covalent modification at a cysteine residue in the central conserved region. Proc. Natl. Acad. Sci. USA **96:**9112–9117.
26. **Levitzki, A., and A. Gazit.** 1995. Tyrosine kinase inhibition: an approach to drug development. Science **267:**1782–1788.
27. **Lin, S. Y., K. Makino, W. Xia, A. Matin, Y. Wen, K. Y. Kwong, L. Bourguignon, and M. C. Hung.** 2001. Nuclear localization of EGF receptor and its potential new role as a transcription factor. Nat. Cell Biol. **3:**802–808.
28. **Lo, H. W., S. C. Hsu, M. Ali-Seyed, M. Gunduz, W. Xia, Y. Wei, G. Bartholomeusz, J. Y. Shih, and M. C. Hung.** 2005. Nuclear interaction of EGFR and STAT3 in the activation of the iNOS/NO pathway. Cancer Cell **7:**575–589.
29. **Lo, H. W., W. Xia, Y. Wei, M. Ali-Seyed, S. F. Huang, and M. C. Hung.** 2005. Novel prognostic value of nuclear epidermal growth factor receptor in breast cancer. Cancer Res. **65:**338–348.
30. **Macara, I. G.** 2001. Transport into and out of the nucleus. Microbiol. Mol. Biol. Rev. **65:**570–594.
31. **Maher, P. A.** 1996. Nuclear translocation of fibroblast growth factor (FGF) receptors in response to FGF-2. J. Cell Biol. **134:**529–536.
32. **Marti, U., and A. Wells.** 2000. The nuclear accumulation of a variant epidermal growth factor receptor (EGFR) lacking the transmembrane domain requires coexpression of a full-length EGFR. Mol. Cell Biol. Res. Commun. **3:**8–14.
33. **Mattaj, I. W., and L. Englmeier.** 1998. Nucleocytoplasmic transport: the soluble phase. Annu. Rev. Biochem. **67:**265–306.
34. **Mayo, L. D., K. M. Kessler, R. Pincheira, R. S. Warren, and D. B. Donner.** 2001. Vascular endothelial cell growth factor activates CRE-binding protein by signaling through the KDR receptor tyrosine kinase. J. Biol. Chem. **276:**25184–25189.
35. **Nachury, M. V., T. J. Maresca, W. C. Salmon, C. M. Waterman-Storer, R. Heald, and K. Weis.** 2001. Importin beta is a mitotic target of the small GTPase Ran in spindle assembly. Cell **104:**95–106.
36. **Ni, C. Y., M. P. Murphy, T. E. Golde, and G. Carpenter.** 2001. γ-Secretase cleavage and nuclear localization of ErbB-4 receptor tyrosine kinase. Science **294:**2179–2181.
37. **Offterdinger, M., C. Schofer, K. Weipoltshammer, and T. W. Grunt.** 2002. c-erbB-3: a nuclear protein in mammary epithelial cells. J. Cell Biol. **157:**929–939.
38. **Peng, H., J. Moffett, J. Myers, X. Fang, E. K. Stachowiak, P. Maher, E. Kratz, J. Hines, S. J. Fluharty, E. Mizukoshi, D. C. Bloom, and M. K. Stachowiak.** 2001. Novel nuclear signaling pathway mediates activation of fibroblast growth factor-2 gene by type 1 and type 2 angiotensin II receptors. Mol. Biol. Cell **12:**449–462.
39. **Rao, V. N., and E. S. Reddy.** 1993. Elk-1 proteins are phosphoproteins and activators of mitogen-activated protein kinase. Cancer Res. **53:**3449–3454.
40. **Reilly, J. F., and P. A. Maher.** 2001. Importin beta-mediated nuclear import of fibroblast growth factor receptor: role in cell proliferation. J. Cell Biol. **152:**1307–1312.
41. **Seol, K. C., and S. J. Kim.** 2003. Nuclear matrix association of insulin receptor and IRS-1 by insulin in osteoblast-like UMR-106 cells. Biochem. Biophys. Res. Commun. **306:**898–904.
42. **Sever, S.** 2002. Dynamin and endocytosis. Curr. Opin. Cell Biol. **14:**463–467.
43. **Stachowiak, E. K., X. Fang, J. Myers, S. Dunham, and M. K. Stachowiak.** 2003. cAMP-induced differentiation of human neuronal progenitor cells is mediated by nuclear fibroblast growth factor receptor-1 (FGFR1). J. Neurochem. **84:**1296–1312.
44. **Stachowiak, E. K., P. A. Maher, J. Tucholski, E. Mordechai, A. Joy, J. Moffett, S. Coons, and M. K. Stachowiak.** 1997. Nuclear accumulation of fibroblast growth factor receptors in human glial cells—association with cell proliferation. Oncogene **14:**2201–2211.
45. **Stachowiak, M. K., P. A. Maher, A. Joy, E. Mordechai, and E. K. Stachowiak.** 1996. Nuclear accumulation of fibroblast growth factor receptors is regulated by multiple signals in adrenal medullary cells. Mol. Biol. Cell **7:**1299–1317.
46. **Strom, A. C., and K. Weis.** 2001. Importin-beta-like nuclear transport receptors. Genome Biol. **2:**3008.1–3008.9.
47. **Suntharalingam, M., and S. R. Wente.** 2003. Peering through the pore: nuclear pore complex structure, assembly, and function. Dev. Cell **4:**775–789.
48. **Vecchi, M., S. Polo, V. Poupon, J. W. van de Loo, A. Benmerah, and P. P. Di Fiore.** 2001. Nucleocytoplasmic shuttling of endocytic proteins. J. Cell Biol. **153:**1511–1517.
49. **Wang, S. C., H. C. Lien, W. Xia, I. F. Chen, H. W. Lo, Z. Wang, M. Ali-Seyed, D. F. Lee, G. Bartholomeusz, F. Ou-Yang, D. K. Giri, and M. C. Hung.** 2004. Binding at and transactivation of the COX-2 promoter by nuclear tyrosine kinase receptor ErbB-2. Cancer Cell **6:**251–261.
50. **Weis, K.** 2002. Nucleocytoplasmic transport: cargo trafficking across the border. Curr. Opin. Cell Biol. **14:**328–335.
51. **Weis, K.** 2003. Regulating access to the genome: nucleocytoplasmic transport throughout the cell cycle. Cell **112:**441–451.

52. **Wells, A., and U. Marti.** 2002. Signalling shortcuts: cell-surface receptors in the nucleus? Nat. Rev. Mol. Cell Biol. **3:**697–702.
53. **Wu, J., M. J. Matunis, D. Kraemer, G. Blobel, and E. Coutavas.** 1995. Nup358, a cytoplasmically exposed nucleoporin with peptide repeats, Ran-GTP binding sites, zinc fingers, a cyclophilin A homologous domain, and a leucine-rich region. J. Biol. Chem. **270:**14209–14213.
54. **Xie, Y., and M. C. Hung.** 1994. Nuclear localization of p185neu tyrosine kinase and its association with transcriptional transactivation. Biochem. Biophys. Res. Commun. **203:**1589–1598.
55. **Yang, J., E. S. Bardes, J. D. Moore, J. Brennan, M. A. Powers, and S. Kornbluth.** 1998. Control of cyclin B1 localization through regulated binding of the nuclear export factor CRM1. Genes Dev. **12:**2131–2143.
56. **Yokoyama, N., N. Hayashi, T. Seki, N. Pante, T. Ohba, K. Nishii, K. Kuma, T. Hayashida, T. Miyata, U. Aebi, et al.** 1995. A giant nucleopore protein that binds Ran/TC4. Nature **376:**184–188.
57. **Zammit, C., R. Barnard, J. Gomm, R. Coope, S. Shousha, C. Coombes, and C. Johnston.** 2001. Altered intracellular localization of fibroblast growth factor receptor 3 in human breast cancer. J. Pathol. **194:**27–34.